International Journal of Research in Engineering, Science and Management
Volume-2, Issue-8, August-2019
www.ijresm.com | ISSN (Online): 2581-5792

Design and Implementation of Dual Input Dual Output Boost Converter

J. Amulya[1], G. S. Srikanth[2]
[1]*M.Tech. Student, Dept. of Electrical & Electronics Engineering, RV College of Engineering, Bengaluru, India*
[2]*Chief, Department of R & D, Arbutus Technologies Pvt. Ltd., Bengaluru, India*

***Abstract*: In the zero emission electric power generation system, Multiple-Input Multiple-output (MIMO) DC-DC converters are useful to obtain the regulated output voltages from several input power sources such as a solar array, wind generator, fuel cell, batteries and so forth. A Dual input Dual Output (DIDO) DC- DC Converter s proposed n this paper with boost topology. This converter s non-isolated, simple n structure with a single inductor and has less number of components compared to the conventional converters. Design and simulation of the converter s presented and results are validated by hardware implementation.**

***Keywords*: DIDO Boost converter, inductor, battery, renewable energy sources.**

1. Introduction

In recent technology, renewable energy sources such as fuel cells, photovoltaic (PV) arrays are increasingly being used in microgrids, automobiles, residential and commercial buildings to develop clean energy without pollution to protect natural environment [1]. In this scenario, Multiple-Input Multiple-Output DC-DC converters are useful to combine several input power sources and to have different output voltage levels and power capacity [2].

In conventional scheme of power transfer in converters, each source delivers power to the load through Single-Input Single-output (SISO) converter as shown in Fig 1(a). In order to integrate of different sources, multiple number of SISO converter has to be employed as represented in Fig 1(b). As the result, it leads to disadvantages like increase in size, weight, cost of the converter. Further, efficiency and reliability also decreases. Hence, Multiple Input Multiple Output (MIMO) converter is implemented to overcome these limitations [3]-[6].

In this paper, Dual Input Dual Output (DIDO) Boost Converter is proposed. The converter has more advantages compared to conventional single input single output (SISO) converters such as, lesser number of components, only one inductor, higher reliability and efficiency [7]-[9]. The block diagram of DIDO converter is shown in Fig 2. The converter consists of two inputs and two outputs. As the converter has two different voltages levels at input, it can be used to interface different energy sources and also different voltage level outputs can be obtained in several applications like, to integrate with multi-level inverter, ventilation system and lightning system in the Electric vehicle. The DIDO converter can also be applied in micro-grids to meet the required load using renewable energy sources as input supply[10], [11].

This paper is about design and implementation of non-isolated Dual Input Dual Output (DIDO) DC-DC boost converter. The converter has two inputs; one is DC supply and another is battery. The input sources not only supply power to the load but also charge the battery. Two outputs of the converter are considered for two different voltage levels.

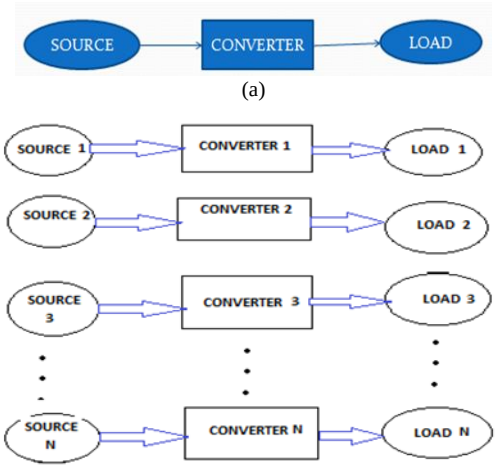

Fig. 1. (a) Block diagram of Single-Input Single-Output (SISO) converter. (b) Representation of multiple number of SISO converters

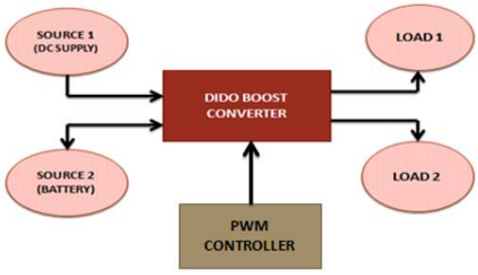

Fig. 2. Block diagram representation of DIDO converter

2. Modes of operation

The circuit diagram of DIDO Boost Converter is shown in Fig. 3. The circuit consists of four MOSFET power switches S_1,

S_2, S_3 and S_4 to control the power flow and output voltages of the converter. V_{in1}, V_{in2} are two input voltage sources and V_{o1}, V_{02} are the two output voltages. V_{in1} is considered as any DC sources like fuel cell, PV solar array, Regulated DC power supply(RPS) etc. V_{in2} has to be considered as battery to show that battery can be charged through converter itself.

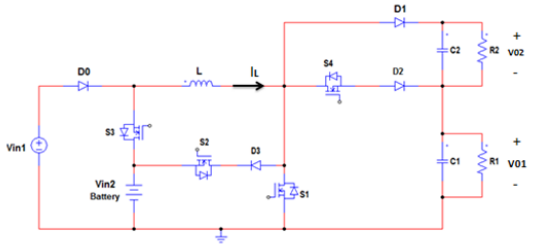

Fig. 3. Circuit Diagram of DIDO Converter

Two power operation modes are defined depending on utilization state of the battery for the converter namely,

1) Battery discharging mode
2) Battery charging mode.

In each mode only three switches of four are active and one switch is inactive. Input source V_{in1} not only supplies loads but also charges V_{in2} (battery).

A. *Battery Discharging Mode*

In battery discharging -operation mode, both input power sources V_{in1} and V_{in2} are responsible for supplying the loads. The switch S_2 is entirely off and switches S_1, S_3 and S_4 are active. S2 and D3 provides battery recharging path in the circuit. Since battery is in discharging mode, battery recharging path is not necessary. Hence switch S2 is made entirely OFF during this period. Regulation of total output voltage V_T ($V_T = V_{01} + V_{02}$) desired value is controlled-by duty ratio of switch S_3. Output voltage V_{01} is controlled by switch S_4. By the regulation of voltages V_T and V_{01}, V_{02}-is also regulated. Gate signals of switches, voltage and current waveform of inductor in discharging switching states (DSS) are shown in Fig.4.

In discharging mode, four switching sates are defined. Switch S_2 is OFF throughout this mode. Four discharging mode switching states are as follows:

1) Discharging Switching State 1(DSS1): Switches S_1, S_3, S4 are ON and S_2 is OFF.
2) Discharging Switching State 2(DSS2): Switches S_1, S_4 are ON and S_2, S_3 are OFF.
3) Discharging Switching State 3(DSS3): Switch S_4 is ON and S_1, S_2, S_3 are OFF.
4) Discharging Switching State 4(DSS4): All switches are OFF.

1) *Discharging Switching State 1 (DSS1)*

In switchingistate1of discharging mode, switches S_1 and S_3 are turned ON. Diodes D1 and D2 are reverse biased since $S_1$is On. Switch S_4 is off. The diode D0 is connected between two input sources to avoid paralleling of them. In this project V_{in1} is considered less than V_{in2} ($V_{in1}<V_{in2}$). As S_3 is ON and $V_{in1}<V_{in2}$ diode D_0 is reverse biased. In this state, V_{in2} charges inductor L, so inductor current increases. Capacitors C_1 and C_2 are discharged and deliver stored energy to load resistances R_1 and R_2 respectively. Equivalent circuit of the converter in this state is shown in Fig. 5.

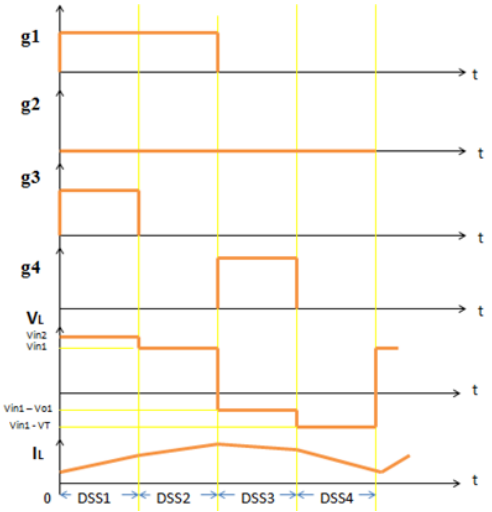

Fig. 4. Waveform of Gate Signals, Inductor Voltage and Inductor Current

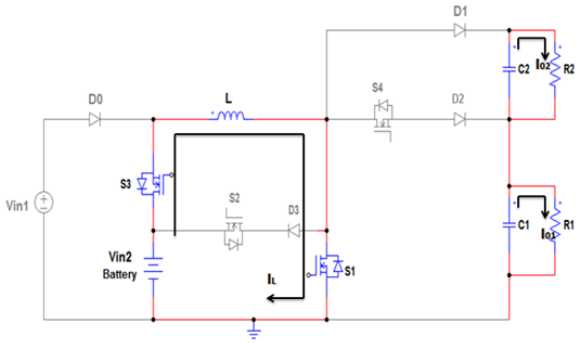

Fig. 5. Switching State1 Operation Circuit in Discharging Mode

The inductor and capacitors equations in this mode are as follows:

$$L \frac{d}{dt} i_L = V_{in2} \quad (1)$$

$$C_1 \frac{dV01}{dt} = -\frac{V01}{R1} \quad (2)$$

$$C_2 \frac{dV02}{dt} = -\frac{V02}{R2} \quad (3)$$

2) *Discharging Switching State 2 (DSS2)*

In state 2 of discharging mode, S_1 is ON and S_3 is off. Since S_1 is on, diodes D_1 and D_2 are reverse biased and also S_4 is OFF. In this operation, V_{in1} charges inductor L, so inductor current rises. The capacitors C_1 and C_2 are discharged and deliver stored energy to load resistances R_1 and R_2 respectively. Equivalent circuit of proposed converter in this state is shown in Fig. 6.

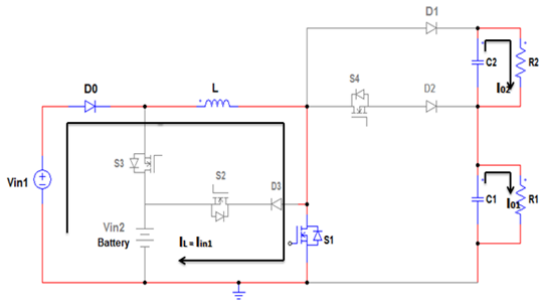

Fig. 6. Switching State 4 Operation Circuit in Discharging Mode

The inductor and capacitors equations in this mode are as follows:

$$L\frac{d}{dt}i_L = V_{in1} \quad (4)$$

$$C_1\frac{dV01}{dt} = -\frac{V01}{R1} \quad (5)$$

$$C_2\frac{dV02}{dt} = -\frac{V02}{R2} \quad (6)$$

3) Discharging Switching State 3 (DSS3)

In this state of operation, switch S_1 is OFF and switch S_3 is still OFF. The switch S_4 is turned on. Diode D_2 is reverse biased. The inductor L is discharged and delivers stored energy to C_1 and R_1 hence inductor current decreased. C_1 is charges and C_2 discharges. Equivalent circuit of converter is shown in Fig.7. The inductor and capacitors equations in this mode are as follows:

$$L\frac{d}{dt}i_L = V_{in1} - V_{01} \quad (7)$$

$$C_1\frac{dV01}{dt} = i_L - \frac{V01}{R1} \quad (8)$$

$$C_2\frac{dV02}{dt} = -\frac{V02}{R2} \quad (9)$$

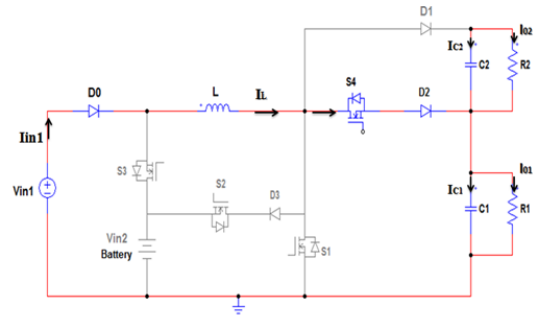

Fig. 7. Switching State3 Operation Circuit in Discharging Mode

4) Discharging Switching State 4 (DSS4)

In state 4 of discharging operation mode, all the switches are OFF. Therefore, diode D2 is forward biased. Inductor L is discharged and delivers stored energy to capacitors C_1 and C_2. In this state capacitors C_1 and C_2 are charged. The equivalent circuit diagram is shown in Fig. 8.

The operational equations of state 4 are,

$$L\frac{d}{dt}i_L = V_{in1} - (V_{01} + V_{02}) \quad (10)$$

$$C_1\frac{dV01}{dt} = i_L - \frac{V01}{R1} \quad (11)$$

$$C_2\frac{dV02}{dt} = i_L - \frac{V02}{R2} \quad (12)$$

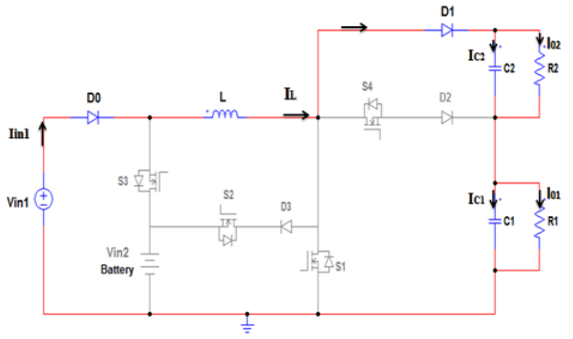

Fig. 8. Switching State 4 Operation Circuit in Discharging Mode

B. Battery charging mode

In battery charging mode, V_{in1} not only supplies power to load but also delivers power to V_{in2}. The switches S_1, S_2 and S_4 are active and switch S_3 is OFF throughout charging mode. Similar to previous operation discharging mode of the converter, for each switch a specific duty is considered depending upon the operation of switches to control the output voltages. S_1 is switched to regulate total output voltage V_T ($V_T = V_{01} + V_{02}$) to desired value and output voltage V_{01} is controlled by switch S_4. By the regulation of V_T and V_{01} the output voltage V_{02} is regulated. In Fig.9, Gate signals of switches and voltage and current waveforms of inductor are shown.

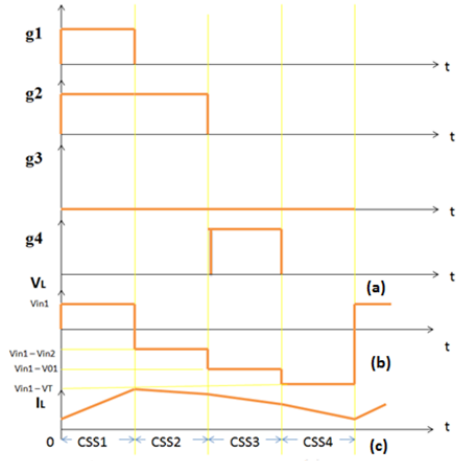

Fig. 9. Waveform of Gate Signals, Inductor Voltage and Inductor Current

According to different switches states, there are four different operations are discussed.

1) Charging Switching State 1(CSS1): Switches S_1, S_2, S_4 are ON and S_3 is OFF.
2) Charging Switching State 2(CSS2): Switches S_2, S_4 are ON and S1, S_3 are OFF.
3) Charging Switching State 3(CSS3): Switch S_4 is ON and S_1, S_2, S_3 are OFF.

4) Charging Switching State 4(CSS4): All switches are OFF.

1) Charging Switching State 1(CSS1)

In this switching state, S_1 is turned ON, so S_2 and S_4 are reverse biased and cannot be turned ON. Diode D_2 is reverse biased. During operation, V_{in1} charges the inductor L, hence inductor current increases. Capacitors C_1 and C_2 are discharged and deliver stored energy to load. Equivalent circuit of converter is shown in Fig.10.

The inductor and capacitors equations in switching sate 1 are,

$$L\frac{d}{dt}i_L = V_{in1} - (V_{01} + V_{02}) \quad (13)$$

$$C_1\frac{dV01}{dt} = i_L - \frac{V01}{R1} \quad (14)$$

$$C_2\frac{dV02}{dt} = i_L - \frac{V02}{R2} \quad (15)$$

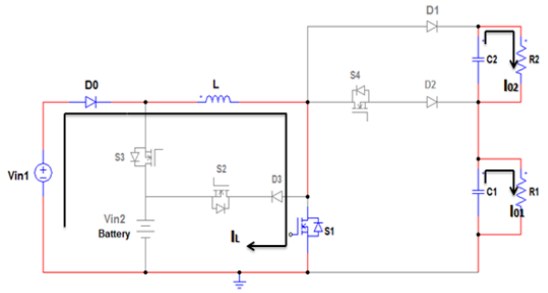

Fig. 10. Switching State 1 Operation Circuit in Charging Mode

2) Charging Switching State 2(CSS2)

In this state, switch S_1 is ON and switch S_2 is also ON. Diode D1 and D2 are reverse biased, consequently S4 is OFF. Since $V_{in1} < V_{in2}$, therefore in this period inductor current decreases and inductor delivers its stored energy to battery (V_{in2}). Capacitors C_1 and C_2 are discharged and deliver stored energy to load resistances R_1 and R_2 respectively. Switching State 2 operation circuit in charging Mode is shown in Fig. 11.The inductor and capacitors equations in this mode are as follows

$$L\frac{d}{dt}i_L = V_{in1} - V_{01} \quad (16)$$

$$C_1\frac{dV01}{dt} = -\frac{V01}{R1} \quad (17)$$

$$C_2\frac{dV02}{dt} = -\frac{V02}{R2} \quad (18)$$

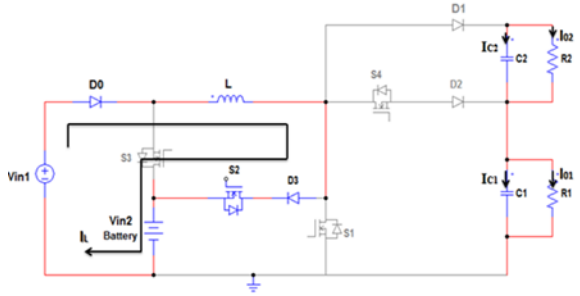

Fig. 11. Switching State 2 Operation Circuit in Charging Mode

3) Charging Switching State 3(CSS3)

In this state, S_1 s OFF and switches S_4 s ON. During the operation, inductor L s discharged and delivers stored energy to C_1 and R_1, thus inductor current is decreased. Capacitors C_1 s charged and capacitor C_2 is discharged and delivers stored energy to load resistance R_2. Equivalent circuit of converter is shown in Fig. 12.

The energy storage elements equations in this mode are as follows:

$$L\frac{d}{dt}i_L = V_{in1} - V_{01} \quad (19)$$

$$C_1\frac{dV01}{dt} = i_L - \frac{V01}{R1} \quad (20)$$

$$C_2\frac{dV02}{dt} = -\frac{V02}{R2} \quad (21)$$

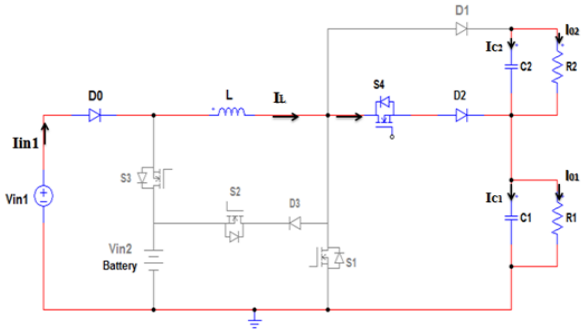

Fig. 12. Switching State 3 Operation Circuit in Charging Mode

4) Charging Switching State 4(CSS4)

In state 4, all the switches are off. Therefore, diode D2 is forward biased. The inductor L is discharged during this state 4 and delivers its stored energy to capacitor C_1 and C_2 and load resistances R_1 and R_2. Capacitors C_1 and C_2 are charged. The circuit diagram is shown in Fig. 13.

Equations of inductor and capacitor in switching state4 are given by,

$$L\frac{d}{dt}i_L = V_{in1} - (V_{01} + V_{02}) \quad (22)$$

$$C_1\frac{dV01}{dt} = i_L - \frac{V01}{R1} \quad (23)$$

$$C_2\frac{dV02}{dt} = i_L - \frac{V02}{R2} \quad (24)$$

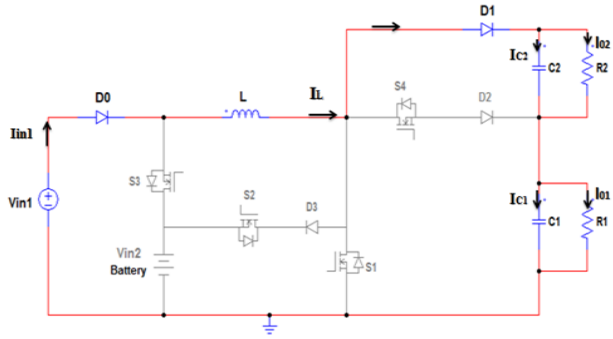

Fig. 13. Switching State4 Operation Circuit in Charging Mode

The Battery discharging mode and Battery charging mode together completes one cycle it is represented with output voltages V_{01} and V_{02} in Fig. 14.

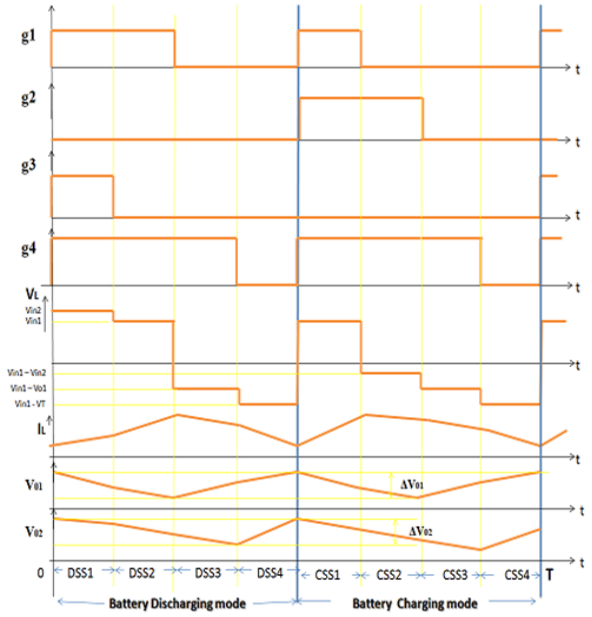

Fig. 14. Complete cycle representation of Discharging and Charging modes of battery with Output voltages

3. Design of the converter

The proposed DIDO converter specifications are tabulated in Table 1. Electrical Specifications of converter are performance limit of the converter. The DIDO Boost converter is designed for load of 40W, with input voltages being 6V and 12V and to obtain output voltages 24V and 40V respectively.

Table 1
Specifications of Converter used for DIDO Converter

Parameter	Values
Input Voltage 1	6V
Input Voltage 2	12V
Output Voltage 1	24V
Output Voltage 2	40V
Power rating	40W
Voltage ripple	5%
Current ripple	20%

Considerations:

- Inductor ripple current Δi_L = 20%
- Output ripple voltage ΔV_c = 5%
- Switching frequency f_s = 20KHz
- Duty ratios of switches, D_1=50%, D_2=25%, D_3= 25%, D_4= 25%
- Output power1 P_{o1}= 20W, Output power2 P_{o2}= 20W

Output power is given by,

$$P_{01} = \frac{(V_{01})^2}{R_1} \quad (25)$$

$$P_{02} = \frac{(V_{02})^2}{R_2} \quad (26)$$

The output resistances R_1 and R_2 are calculated from equations (25) and (26) is given by,

$$R_1 = \frac{(V_{01})^2}{P_{01}} \quad (27)$$

$$R_1 = \frac{(24)^2}{20}$$

$$R_1 = 28.8\Omega$$

Standard resistance value of R_1 is chosen as $R_1 = 50\Omega$

Similarly,

$$R_2 = \frac{(V_{02})^2}{P_{02}} \quad (28)$$

$$R_2 = \frac{(40)^2}{20} = 80\Omega$$

Standard resistance value of R_2 is chosen as $R_2 = 100\Omega$

The inductor ripple current Δi_L is assumed to be 20% and it is given by,

$$\Delta i_L = 20\%\ I_L \quad (29)$$

Where, I_L is the average inductor current and it is equal to output current I_o in boost converter ($I_L = I_0$).

Output current is found by formula (30),

$$P_{01} = (I_{01})^2 * R_1 \quad (30)$$

Therefore, output current1 I_{01} is given by,

$$I_{01} = \sqrt{\frac{P_{01}}{R_1}} \quad (31)$$

$$I_{01} = \sqrt{\frac{20}{50}}$$

$$I_{01} = 0.63A$$

Similarly, Output current 2 I_{02} is given by,

$$I_{02} = \sqrt{\frac{P_{02}}{R_2}} \quad (32)$$

$$I_{02} = \sqrt{\frac{20}{100}}$$

$$I_{02} = 0.443A$$

Average inductor current is calculated applying KCL at node in Fig. 15.

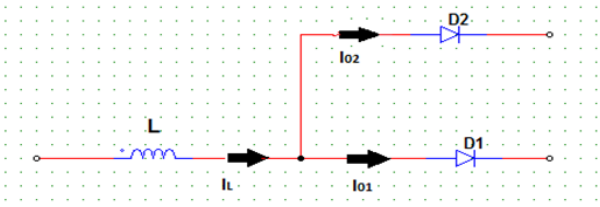

Fig. 15. Average Inductor Current Flow

Applying KCL at node,

$$I_L = I_{01} + I_{02}$$

$$I_L = 0.63 + 0.443$$

$$I_L = 1.07A$$

From equation (29),
$\Delta i_L = 20\% * I_L$
$\Delta i_L = 0.2 * 1.07$
$\Delta i_L = 0.214A$

Maximum inductor current I_M is given by (33),

$$I_M = Io + (\Delta i_L/2) \quad (33)$$

$I_M = 1.07+ (0.214/2) = 1.17A$

For inductor core, Ferrite E core EE30 is selected.
Inductance L is given by (34),

$$L = \frac{V_{in1}(V_{OT}-V_{in1})}{\Delta i_L * f_s * V_{OT}} \quad (34)$$

$$L = \frac{6(64-6)}{0.214*20*10^3*64}$$

L = 1.27mH

Number of turns N is calculated using equation,

$$N = \frac{L * I_M}{A_C * B_M} \quad (35)$$

Referring EE30 core parameters Area of core A_C and maximum flux density B_M are chosen. Applying A_C and B_M in equation (35),

$$N = \frac{1.27*10^{-3}*1.17}{0.4*60*10^{-6}}$$

N = 61.9 = 62 turns

The capacitances C1 and C2 are,

$$C1 = \frac{D_1}{R_1(\Delta VC1/Vo1)fs} \quad (36)$$

$$C2 = \frac{D_1}{R_2(\Delta V_{C2}/Vo2)fs} \quad (37)$$

Considering the voltage ripple to be 5%, C1 and C2 are
C1 = 240µF
C2 = 200 µF

The final designed values of the components are tabulated in table 2.

Table 2
Design Values of DIDO Boost Converter

Parameter	Values
Inductor L	1.2mH
Capacitor C_1	240uF
Capacitor C_2	200uF
Resistance R_1	50Ω
Resistance R_2	100Ω

4. Simulation of the Converter

The simulation circuit of DIDO Boost Converter is illustrated in Fig. 16. The voltmeter is connected across load to measure output voltage of the converter. The simulation s carried out n MATLAB. In the simulation of DIDO converter, the input voltage of 12V and 6V are boosted to 24V and 40V. The output results of simulation are shown in Fig. 17. The output voltages of 24V and 40V are obtained and it is shown in Fig. 17 (a) and (b). The battery charging and discharging is represented in Fig. 17 (c).

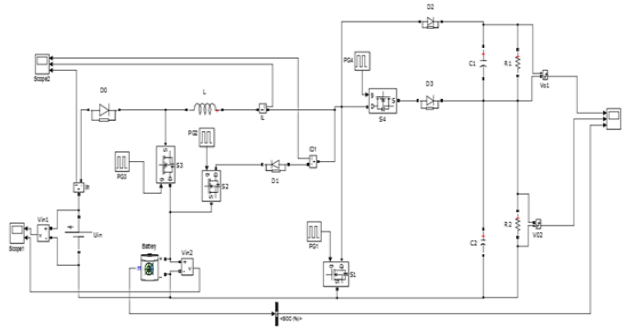

Fig. 16. DIDO Converter Simulation Circuit

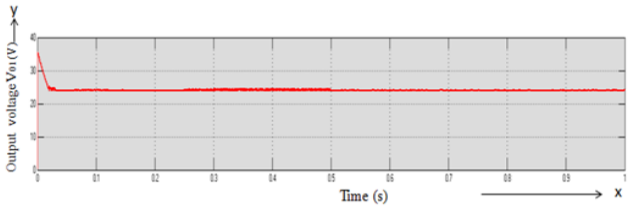

(a) Output Voltage V01 of 24V

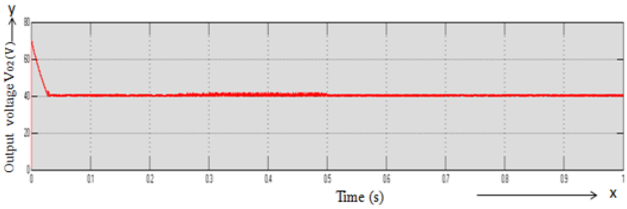

(b) Output Voltage V02 of 40V

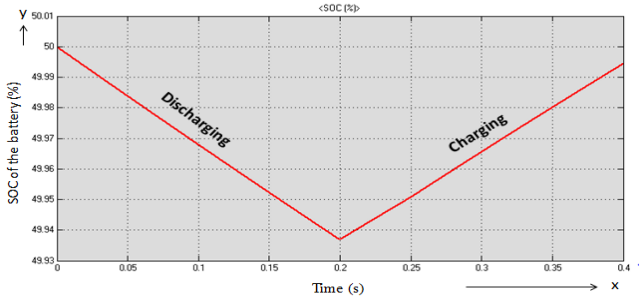

(c) SOC of Battery

Fig. 17. Output voltages of 24V and 40V and SOC of the battery

5. Hardware Implementation

The hardware implementation of DIDO Converter involves power supply circuit and PWM controller circuit. For the design specification of input V_{in1}=6V, V_{in2} = 12V and output V_{o1}=24V and V_{02}=40V is successfully implemented. The hardware implementation of DIDO converter is shown in Fig. 18.

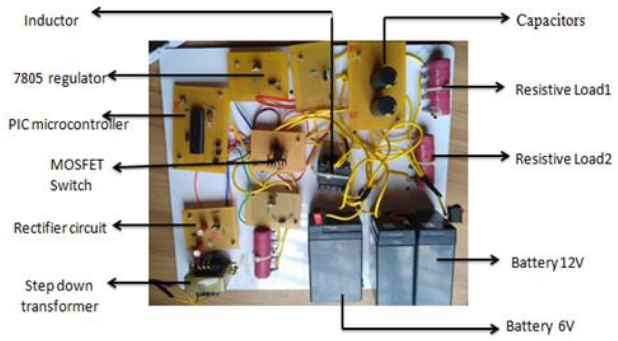

Fig. 18. Hardware Implementation

Output voltages measured across two loads are shown in Fig. 19 and Fig. 20 respectively. Fig Gate pulses given for switches are represented in Fig. 21 (a), (b), (c) and (d) for switches S2, S3, S1 and S4 respectively.

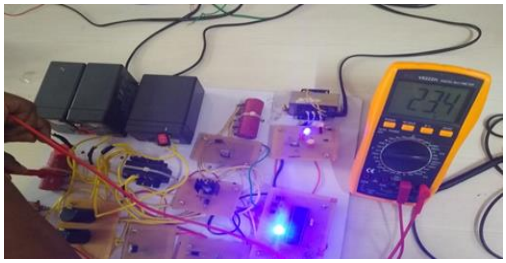

Fig. 19. Output Voltages V01

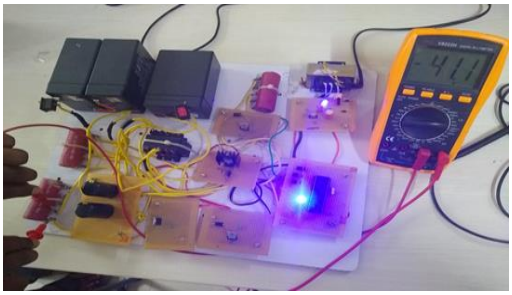

Fig. 20. Output Voltages V02

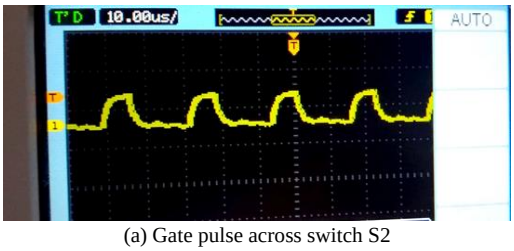

(a) Gate pulse across switch S2

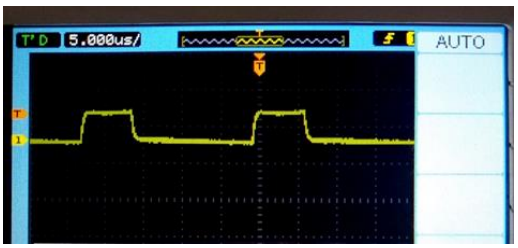

(b) Gate pulse across switch S3

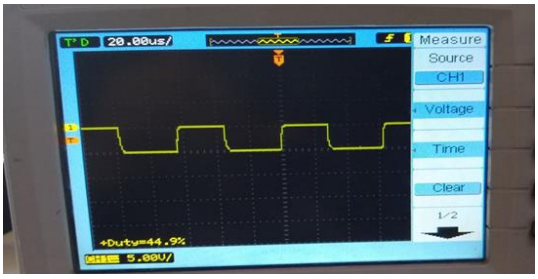

(c) Gate pulse across switch S1

(d) Gate pulse across switch S4

Fig. 21. Gate pulse measured across the switch S2, S3, S1 and S4

6. Conclusion

DC-DC converters are widely used to efficiently produce a regulated voltage from the source. Conventionally, to supply to different loads and to obtain energy from different sources, discrete power converters of Single input single output (SISO) are implemented and regulated separately. As the result, cost, size and weight of converter increased and further, efficiency and reliability also reduced. Therefore, converters with Multiple-inputs and Multiple-outputs (MIMO) are introduced. Hence, in recent technologies, renewable energy sources are widely incorporated in DC-DC converters as input energy source. Multi-Input Multi-Output converters are most used converters and play a crucial role in incorporating different energy sources with less number of components.

In this project work, a 40W Dual-Input Dual-Output Converter with boost topology s designed for battery discharging and charging modes. Providing 6V and 12V lead acid batteries as input sources, the converter of s simulated at a switching frequency of 20 kHz and implemented to obtain output voltages of 24V and 40V. n both battery discharging and charging modes, out of four MOSFET switches only three switches are ON and one is OFF. Each switching state was conducted for equal duration and according to this the operation, duty ratios are considered. The MOSFET switches are fired by PWM pulses obtained by programming PIC16F877A microcontroller. Voltage and current waveforms of each circuit element s studied, and the data obtained s used for component selection, to implement the hardware.

References

[1] W. Li and X. He, "Review of Nonisolated High-Step-Up DC/DC Converters in Photovoltaic Grid-Connected Applications," in *IEEE Transactions on Industrial Electronics*, vol. 58, no. 4, pp. 1239-1250, April 2011.

[2] M. H. Taghvaeea, M. A. M. Radzia, S. M. Moosavainb, Hashim Hizama and Hamiruce Marhabana, “A current and future study on non-isolated DC–DC converters for photovoltaic applications,” *Renewable and Sustainable Energy Reviews*, vol. 17, pp. 216-227, January 2013.

[3] Z. Rehman, I. Al-Bahadly and S. Mukhopadhyay, "Dual input-dual output single inductor dcdc converter for renewable energy applications," *2015 International Conference on Renewable Energy Research and Applications (ICRERA)*, Palermo, 2015, pp. 783-788.

[4] A. A. de Melo Bento, D. A. Acevedo-Bueno and E. R. Cabral da Silva, "Dual input dual output single switch DC-DC converter for renewable energy applications," *2016 IEEE Energy Conversion Congress and Exposition (ECCE)*, Milwaukee, WI, 2016, pp. 1-8.

[5] B. L. Nguyen, H. Cha, T. Nguyen and H. Kim, "Family of Integrated Multi-Input Multi-Output DC-DC Power Converters," *2018 International Power Electronics Conference (IPEC-Niigata 2018-ECCE Asia)*, Niigata, 2018, pp. 3134-3139.

[6] F. Ahmad, A. A. Haider, H. Naveed, A. Mustafa and I. Ahmad, "Multiple Input Multiple Output DC to DC Converter," *2018 5th International Multi-Topic ICT Conference (IMTIC)*, Jamshoro, 2018, pp. 1-6.

[7] H. Matsuo, Wenzhong Lin, F. Kurokawa, T. Shigemizu and N. Watanabe, "Characteristics of the multiple-input DC-DC converter," in *IEEE Transactions on Industrial Electronics*, vol. 51, no. 3, pp. 625-631, June 2004.

[8] H. Shao, X. Li, C. Tsui and W. Ki, "A Novel Single-Inductor Dual-Input Dual-Output DC–DC Converter with PWM Control for Solar Energy Harvesting System," in *IEEE Transactions on Very Large Scale Integration (VLSI) Systems*, vol. 22, no. 8, pp. 1693-1704, Aug. 2014.

[9] H. Lee and P. Chen, "A single-inductor dual-input dual-output (SIDIDO) power management with sequential pulse-skip modulation for battery/PV hybrid systems," *2016 IEEE Asian Solid-State Circuits Conference (A-SSCC)*, Toyama, 2016, pp. 293-296.

[10] H. Zhang, L. Harnefors, X. Wang, J. Hasler and H. Nee, "SISO Transfer Functions for Stability Analysis of Grid-Connected Voltage-Source Converters," *2018 International Power Electronics Conference (IPEC-Niigata 2018 -ECCE Asia)*, Niigata, 2018, pp. 3684-3691.

[11] A. A. Nilangekar and R. G. Kale, "Design and development of electric vehicle battery charging using MIMO boost converter," *2016 Online International Conference on Green Engineering and Technologies (IC-GET)*, Coimbatore, 2016, pp. 1-6.